

Title	Field Emission Properties of Periodic Porous Carbon with Various Pore Size
Author(s)	Ojima, Masayoshi; Hiwatashi, Shinji; Araki, Hisashi et al.
Citation	電気材料技術雑誌. 14(2) p.81-p.84
Issue Date	2005-07-15
oaire:version	VoR
URL	<a href="https://hdl.handle.net/11094/76811">https://hdl.handle.net/11094/76811</a>
rights	
Note	

*Osaka University Knowledge Archive : OUKA*

<https://ir.library.osaka-u.ac.jp/>

Osaka University

## Field Emission Properties of Periodic Porous Carbon with Various Pore Size

Masayoshi Ojima<sup>1</sup>, Shinji Hiwatashi<sup>1</sup>, Hisashi Araki<sup>1</sup>, Akihiko Fujii<sup>1</sup>,  
Katsumi Yoshino<sup>1,2</sup> and Masanori Ozaki<sup>1</sup>

*1 Department of Electronic Engineering, Graduate School of Engineering, Osaka University,  
2-1 Yamadaoka, Suita-shi, Osaka 565-0871, Japan  
Tel: +81-6-6879-7759, Fax: +81-6-6879-7774*

*E-mail: mojima@ele.eng.osaka-u.ac.jp*

*2 Center for University-Industry Cooperation, Shimane University,  
Matsue, Shimane 690-0816 Japan*

Porous carbons with nano-pores have attracted much attention due to their potential applications such as the electrodes of a fuel cell, hydrogen storage, and electric double-layer capacitors [1-4].

Carbon inverse opals with various pore sizes have been fabricated by a template method using synthetic opals, and their pore sizes were controllable in nano-order [5-7]. These materials were expected to have unique and useful properties as optical and electrical device, because they had a periodic porous nano-structure with a periodicity of the order of optical wavelengths.

The carbon-based electron field emitters have won worldwide attention as a new electron source for a flat panel display [8]. Many researchers had an interest on carbon nano tube arrays as an excellent source for field emission (FE) [9-11]. However, fabrication processes of the controlled carbon nano tube arrays were not so easy and expensive. The porous carbon fabricated by the template method has a large domain with periodical and regular voids, and its void density is controllable. Therefore we can easily control the emission sites density. In addition, fabrication processes of the porous carbon are very easy. Strategy to utilize the carbon inverse opals as the field emitter has never been studied to our knowledge. In this study, the FE characteristics in the several porous carbons are studied and the effective emitting area is discussed.

Synthetic opals were fabricated by sedimentation of the suspension of monodispersed SiO<sub>2</sub> spheres of 74, 120, 300 and 550 nm in diameter and sintered at 700–900°C. These opals contain interconnecting octahedral voids whose diameters depend on the diameter of SiO<sub>2</sub> spheres. Pristine products were prepared by infiltrating starting materials, phenolic resin, into the voids in synthetic opals and then pyrolyzing them at 600°C in high-purity Ar atmosphere for carbonization of samples, and subsequently the SiO<sub>2</sub> spheres in the products were removed by immersing into the aqueous solution of hydrofluoric acid. These samples were pyrolyzed at 1100°C for one hour in a high-purity Ar atmosphere again.

Electron microscope images of the morphology of samples were obtained by a scanning electron microscope (SEM) (S-5000, Hitachi) and a transmission electron microscope (TEM) (H-8100, Hitachi).

The FE measurements were performed for the porous carbon as an emitter in a high vacuum chamber. We used a tungsten probe with a diameter of 500  $\mu\text{m}$  as an anode. The cross-sectional area of the anode was  $1.96 \times 10^{-7} \text{ m}^2$ . FE current density-electric field characteristics were studied for various distances ( $Z$ ) between the anode and the porous carbon.

Figure 1 (a) and (b) shows the SEM images of the porous carbon prepared from SiO<sub>2</sub> spheres of 550 and 120 nm in diameter, respectively. These figures revealed that the periodicity and therefore the size of voids were approximately consistent with the diameter of spheres of synthetic opals.

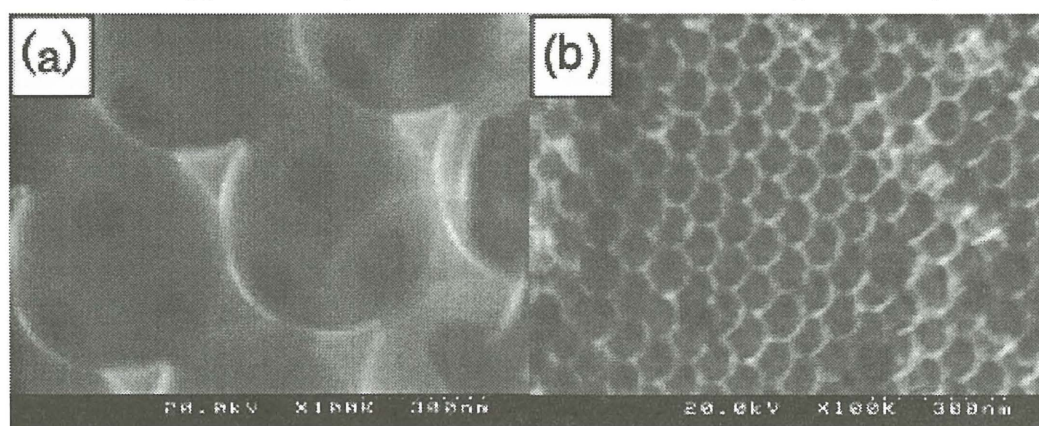


Fig. 1. SEM images of porous carbon prepared from SiO<sub>2</sub> sphere of (a) 550 nm and (b) 120 nm

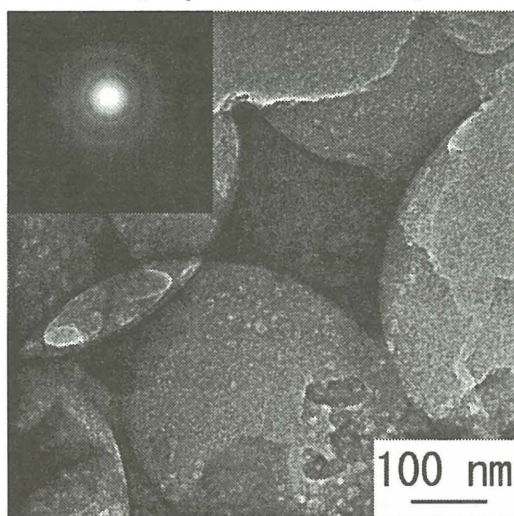


Fig. 2. TEM image and the electron diffraction pattern of porous carbon

Figure 2 shows the TEM image and the electron diffraction pattern of the porous carbon with 550 nm pore size. The TEM image is rather complicated but can be explained as one corresponding to a well arranged three-dimensional pore structure. The electron diffraction exhibits halo-pattern, and therefore demonstrates that crystalline structure of the porous carbon pyrolyzed at 1100°C is amorphous.

Figure 3(a) shows the FE current density – electric field characteristics for various porous carbons with different pore sizes ranging between 74 and 550 nm as mentioned above when  $Z = 40 \mu\text{m}$ . Threshold electric field was decreased with decreasing the pore size. These J–E characteristics seem to be saturated in a current density range of  $J > 10^{-3} - 10^{-5} \text{ (A/cm}^2\text{)}$ . Similar phenomena were also observed in characteristics from the carbon nano tube array [12,13].

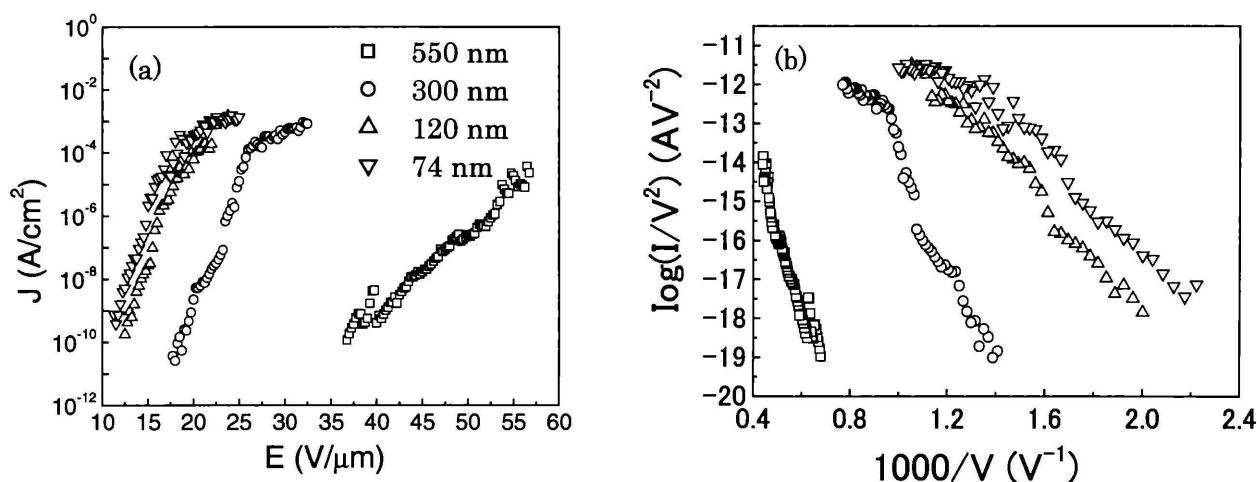


Fig. 3. (a) FE current density–electric field characteristics for the electrodes distance of 40 μm  
(b) FN plots of the current–voltage characteristics

These current density–electric field characteristics were analyzed by the Fowler–Nordheim (FN) equation for FE. The emission current density  $J$  as a function of the local electric field at the emitter surface  $F$  is given by  $J = (AF^2/\phi) \exp(-B\phi^{3/2}/F)$  (A m<sup>-2</sup>) with  $A = 1.56 \times 10^{-10}$  (A V<sup>-2</sup> eV),  $B = 6.83 \times 10^9$  (V eV<sup>-3/2</sup> m<sup>-1</sup>), and  $\phi$  the work function. Figure 3 (b) shows the FN plots for the observed current–voltage characteristics. Data points in a low voltage range of the FN plots were approximately on a straight line, which indicates that the analysis of the data utilizing FN equation is reasonable. From the slope and the ordinate intercept of the straight line we estimated the field enhancement factor and the effective emission area with a work function taken equal to that of graphite (5 eV). It was found that with decreasing pore size both the field enhancement factor and the effective area became larger.

FE is expected to be caused at the site of the most concentrated electric field in front of the pore surface. Site A in Fig.4 (a) corresponds to a sharp edge formed in the boundary of the neighboring pores, and the edge in the site A is shown schematically in Fig.4 (b) by illustrations of the front view and the cross-sectional view in the boundary of Fig.4 (a). Therefore site A is the most promised candidate for the emission sites. There are six sites like site A located in each pore. It is suggested that the area of site A was not change for all pore size, and FE was caused mainly at the sharp edge in the boundary of the pores. With decreasing pore size (diameter of the pore size;  $r$ ) the total number of site A in a unit area increase in proportional to  $r^{-2}$ , which coincide with the result of FN plots.

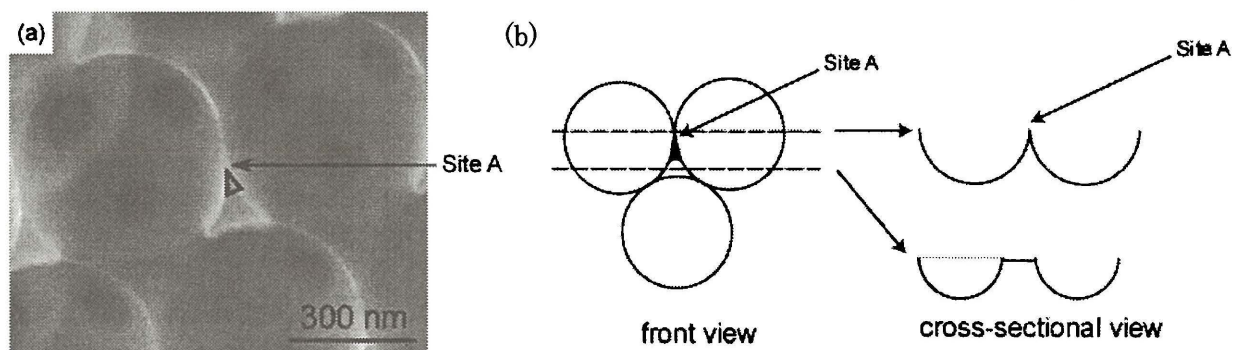


Fig. 4. Emission site of porous carbon



In conclusion, periodic nano-porous carbons having several pore sizes were prepared using synthetic opals. Then, we demonstrated excellent field emission characteristic of the periodic nano-porous carbon and indicated that the main emission site is the sharp edge formed in the boundary of the neighboring pores, and density of the emission site increased proportionally to the pore numbers per unit surface area.

The authors would like to express sincere thanks to Dr. T. Nakayama and Prof. K. Niihara for the use of facilities of the electron microscopy.

#### Reference

- [1] H. Take, T. Matsumoto and K. Yoshino: *Synth. Met.* **135** (2003) 731.
- [2] S. Shiraishi, H. Kurihara, H. Tsubota, A. Oya, Y. Soneda and Y. Yamada: *Electrochem. Solid-State Lett.* **4** (2001) A5.
- [3] S. Han, Y. Yun, K.-W. Park, Y.-E. Sung and T. Hyeon: *Adv. Mater.* **15** (2003) 1922.
- [4] J. S. Yu, S. Kang, S. B. Yoon and G. Chai: *J. Am. Chem. Soc.* **124** (2002) 9382.
- [5] A. A. Zakhidov, R. H. Baughman, Z. Iqbal, C. Cui, K. Khayrullin, S. O. Dantas, J. Marti and V. G. Ralchenko: *Science* **282** (1998) 897.
- [6] K. Yoshino, H. Kajii, Y. Kawagishi, M. Ozaki, A. A. Zakhidov and R. H. Baughman: *Jpn. J. Appl. Phys.* **38** (1999) 4926.
- [7] H. Take, T. Matsumoto, S. Hiwatashi, T. Nakayama, K. Niihara and K. Yoshino: *Jpn. J. Appl. Phys.* **43** (2004) 4453.
- [8] A. A. Talin, T. E. Felter, T. A. Friedmann, J. P. Sullivan and M. P. Siegal: *J. Vac. Sci. Technol. A* **14** (1996) 1719.
- [9] W. A. de Heer, A. Chatelain and D. Ugrate: *Science* **270** (1995) 1179.
- [10] J. M. Bonard, J. P. Salvetat, T. Stockli, W. A. de Heer, L. Forro, and A. Chatelain: *Appl. Phys. Lett.* **73** (1998) 918.
- [11] S. Fan, M. G. Chapline, N. R. Franklin, T. W. Tombler, A. M. Cassell, and H. Dai: *Science* **283** (1999) 512.
- [12] H. Araki, T. Katayama and K. Yoshino: *Appl. Phys. Lett.* **79** (2001) 2636.
- [13] K. Kamide, H. Araki and K. Yoshino: *Jpn. J. Appl. Phys.* **42** (2004) 1539.